Targeting Marine Plastic Pollution With Numerical Data Modeling: Predicting Plastic Transport in Massachusetts Bay Through Flow Map Composition

Serena Zhao

Abstract

Marine plastic pollution is a serious and growing problem today. Currently, there are approximately 5.25 trillion pieces of plastic in the ocean, and this amount is expected to increase over time. Plastics polymers enter the oceans through three main source types - point sources, coastal sources, waterways - and degrade slowly, only fragmenting into smaller and less detectable micro- and nanoplastics with exposure to sunlight and wave action. Thus, it is important that marine plastic pollution is removed as quickly as possible, which requires accurate understanding and predictions of the transport of plastic particles in the ocean. This study turned to numerical modeling to address this. An existing passive transport model, which utilized a novel, computationally efficient composition-based advection method for Lagrangian transport, was modified to forecast and backcast passive plastic transport by implementing various plastic source concentration cases. This modified model was applied to 20-day and 5-day Navier-Stokes current simulations in Massachusetts Bay, MA to successfully simulate plastic movement within the oceanic area. Seven initial source cases were modeled: uniform coastline source; point source in the ocean; Merrimack River discharge; Charles River discharge; combined river discharge with weighted concentrations based on river flow output; uniform coastline source and river sources; and total coastline and offshore uniform source. Results concluded characteristics of plastic flow in the area: *i*) a clear accumulation of plastic in and around Boston Harbor is present; *ii*) Cape Cod Bay appears to be self-clearing, with a consistent lack of particles that remain within in it by the end of the 20 days; *iii*) plastics originating from river sources first cluster around the river mouth, then disperse quickly; *iv*) point sources tend to remain clustered initially in travel through time and disperse slightly overtime. By concluding such findings, the model is able to direct cleanup efforts through both forecasting and backcasting of plastic pollution, thus targeting accumulations and sources. The flexibility of the model is further increased by the ability to generalize it to other forms of passive transport (*eg.* fish larvae of invasive species) and applied to other oceanic regions. Additional factors influencing oceanic plastic movement (*eg.* wind drag, settling, fragmentation) can be incorporated to further enhance the accuracy, efficiency, and versatility of the model.

1 Introduction

1.1 Motivation

The ubiquity of plastics in today's world is evidenced by the abundance of plastic litter in the environment, causing serious and worsening pollution. Plastics were first introduced in the early twentieth century, but the presence of plastic particles in the ocean was only first reported by scientists in the 1970's, when global production was less than 50 million metric tons. Since 1950, global plastic production has been increasing exponentially: 311 million metric tons were produced in 2014 and a projected 850 million metric tons will be produced annually by 2050 [1, 2]. This rapid growth in plastic use owes itself, in large part, to the immense popularity of plastic components and intense consumption of disposable plastic packaging in a wide variety of industries today. Of the annual global plastic production mass, more than one-third of that amount is used to produce disposable plastic packaging, which is discarded within one year of production [1]. About 85% of total plastics demand consists of seven commodity thermoplastics, used in almost all market sectors [2]. Unfortunately, while the use of plastics has become more prevalent, it is clear that plastic-recycling infrastructure and technology have not. In Europe, only 30% of postconsumer plastics were recycled in 2014; in the United States, this number drops to 8.8% and is likely even lower for many developing countries [2]. This insufficiency in recycling efforts leads to serious environmental consequences, as much of the plastic is often discarded and accumulates in the oceans. Currently, an estimated 60-80% of all marine debris is plastic, and plastic is more abundant than plankton by a ratio of over 6:1 [1].

Plastics are a class of synthetic, hydrocarbon-based polymers typically derived from fossil fuels. During production, plastics are enhanced with additives to improve their performance and appearance, resulting in their desirable properties such as abundant forms, strength, durability, light weight, and electrical insulation. These properties not only increase the versatility and, thus, the popularity of plastics in the modern world, but also contribute to their persistence in the environment. Today, plastics are extremely resistant to biodegradation and are easily transportable by wind and water, leading to their widespread marine distribution [2].

Most marine plastics originate from landfills, litter, and discarded fishing and aquaculture gear

and other plastic materials from boats. Only a small minority of plastic wastes on land are recycled or incinerated, with most discarded into landfills or littered into the environment [3]. As a result, enormous volumes of plastic waste are kept intact in the environment, and a large portion of this eventually enters the oceans through runoff, local bodies of water emptying in oceans, coastal deposits, excess accumulations, and general poor management of plastic waste deposits on land. In addition, marine vessels frequently discard fishing gear, aquaculture materials, and other plastic waste directly into the ocean, contributing to the abundance of dangerous pollution such as "ghostnets" [3]. Once in the ocean, plastic particles are exposed to solar radiation and wave action, resulting in their breakdown via photodegradation and fragmentation. The weathering of plastic fragments generates microplastic and nanoplastic particles that are not only difficult to detect and remove, but also especially damaging for organismal and human health [4]. Marine plastics pose serious threats to environmental, human, and organismal health as a result of interactions such as entanglement, ingestion, obstruction, chemical leaching, and toxic bioaccumulation [2]. Because these particles simultaneously persist and fragment, plastics in the ocean become more widespread and difficult to remove with passing time. Thus, to reduce treatment costs and environmental damage, more efficient and targeted removal methods are needed. To achieve this, numerical modeling of ocean dynamics could be used to predict plastic transport and direct cleanup efforts.

1.2 Passive Advection Modeling

The transport of passive particles, or particles whose motion depends on external factors and not independent movement, in atmospheric and ocean dynamics is governed by the advection equation [5]. In most practical situations, advective fluid transport is affected by external factors and processes such as diffusion, reaction processes, and properties of the advected passive particles. Advective transport itself is governed by the following classic partial differential equation (PDE), which models change in multivariable functions using one or more partial derivatives, [5]

$$\frac{\partial \rho(x,t)\alpha(x,t)}{\partial t} + \nabla \cdot (\rho(x,t)v(x,t)\alpha(x,t)) = 0. \tag{1}$$

In equation (1), α is the 'tracer', *i.e.* the scalar quantity representing the particle whose transport

is to be modeled; v is the specified dynamic velocity field on which advection is simulated; ρ is the density of the fluid; and *(x, t)* denotes the spatial and temporal coordinates of the specific particle studied. To solve for the solution $\alpha(x, t)$, simple analytical methods can be used only when the velocity field has well-defined initial and boundary conditions. However, in most real-world cases, this does not hold true and the equation must be solved numerically to examine the evolution of the tracer. This presents difficulties with large, realistic problems, as numerical diffusion lowers accuracy and computational challenges result. [5]

Two different approaches exist to model particle advection, namely the Eulerian and the Lagrangian perspectives. In Eulerian modeling, flow is studied in static "boxes" through which particles move, and the focus rests on comparing particle inflow and outflow in each "box" to determine overall advective patterns. In Lagrangian modeling, the trajectories of individual particles are traced as they move through time and space. There is no advection term describing mass flow across grid boundaries, since the grid deforms with material flow and volume changes; thus, conservation equations for mass, momentum, and energy are simple and can be efficiently solved. Moreover, boundary conditions are easily imposed and material interfaces are smoothly tracked. Collectively, all particle movements follow Lagrangian Coherent Structures (LCS), which are computationally derived and direct the convergence and divergence of flow trajectories. [6] Hence, while Eulerian models are popular for their use of a fixed reference grid, Lagrangian models are more computationally efficient compared to Eulerian models, especially as dimensions of the target region increases [7]. Prants et al. (2011) simulated surface transport and mixing of water masses in the Japan Sea using Lagrangian trajectories computed for particles in a velocity field generated by a numerical circulation model. The resulting map of LCSs revealed mesoscale eddies and their structures, different phases of coastal flow, and particle trajectories on a large scale. [8]

1.3 Goals of Study

Recent research efforts to address pollution control and remediation have been directed towards the modeling of passive particle trajectories for predictive and preventative purposes. Lebreton et al. (2018) predicted and quantified the mass of the Great Pacific Garbage Patch, concluding that the patch is increasing exponentially in size. The numerical model was calibrated with data from multi-

vessel and aircraft surveys, utilizing Lagrangian forecasting reinforced with real-world observations [3]. Liubartseva et al. (2018) created a 2D Lagrangian model of plastics in the Mediterranean which focused on stochastic, or randomized, beaching and sedimentation of plastics. Substantial accumulation of plastics on coastlines and sea bottom, as well as problematic contaminated areas, were identified [9]. Because regions have different characteristics that must be accounted for in accurate models, numerical models such as these must be continuously altered and tailored to fit different target regions, prompting continuous research.

This work aimed to develop a model of plastic transport in Massachusetts Bay, MA (figure 1) for forecasting with special focus on realistic source regions as an initial condition. An existing Lagrangian passive transport model [5], using a composition-based advection method, was modified to incorporate source location and concentration as initial conditions, representing the real-world sources of plastic particles. The model was run for datasets of two different time periods and resulting flow patterns were compared and analyzed for general trends.

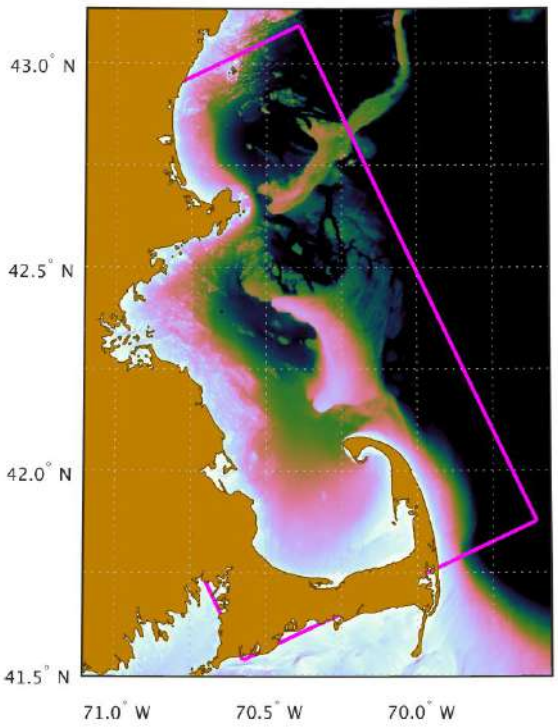

Figure 1: Region modeled includes Massachusetts Bay, Boston Harbor, and Cape Cod Bay. [10]

2 Methodology

2.1 Overview

An existing model for passive transport from the Multidisciplinary Simulation, Estimation, and Assimilation System (MSEAS) Group, MIT, which utilized a composition-based advection method developed by Chinmay S. Kulkarni and Pierre F. J. Lermusiaux [5], was modified to incorporate 7 source condition cases. Simulated Navier-Stokes current velocity fields of Massachusetts Bay, MA, were then generated (by the MSEAS Group, MIT) for two time periods: June 6, 2001 through June 26, 2001 and July 25, 2019 through July 30, 2019. The 2001 dataset is of lower resolution but longer duration than the 2019 dataset. This allows for a comparison of model results with varying resolutions and over different time periods. This study focused on the forecasting function of the model: diagrams of plastic concentration distribution were calculated at different times during both time periods, generating a progression of plastic movement. Resulting trends in particle movement were analyzed to draw conclusions of general plastic flow patterns in Massachusetts Bay.

2.2 Composition-Based Advection Method [5]

2.2.1 Problem Statement

In this section, the governing equation is defined. Let α denote the value of the tracer whose advection is to be studied; ρ denote density of fluid flow; v denote velocity and *(x, t)* denote spatial and temporal conditions over t $\in$ [0, T], the time interval of interest. α_0 denotes initial tracer concentration at a specific spatial coordinate x. Then, assuming an incompressible velocity field ($\nabla \cdot v = 0$), the transport of a passive tracer α defined per unit mass of the transporting fluid can be modeled with,

$$\begin{cases} \frac{\partial \alpha(x,t)}{\partial t} + v(x,t) \cdot \nabla \alpha(x,t)) = 0 \\ \alpha(x,0) = \alpha_0(x) \end{cases} \tag{2}$$

The goal is to compute the tracer field α(x, t) for all $0 \leq t \leq T$, by numerically solving equation (2) over a discretized spatio-temporal domain. The spatial domain is discretized into distinct nodes, with a spacing of Δx along each direction, and the temporal domain is discretized into distinct

intervals of duration Δt.

2.2.2 Flow Maps of Tracer Advection

Flow maps describe fluid movement from a given start time 0 to a given end time T, mapping each particle's initial position to its final position in a defined region under the advective action of the corresponding velocity field v during that time interval, $[0,\ T]$. In essence, flow maps describe where fluid and passive particles at a location will be after a certain amount of time, given that their movement is influenced only by an existing velocity field. The inherent benefit of computing flow maps for tracer advection is that the cost of computing one flow map is equivalent to that of directly computing tracer advection for one initial spatio-temporal condition. As such, once the flow map is generated, advected tracer values can be easily computed since corresponding tracer values do not change as tracer parcels are passively transported. Thus, by simply attaching tracers to the initial advecting positions on flow maps, tracer values can be followed to final advecting positions.

The transport of an individual fluid parcel, located at x_0, and its associated passive tracer with value $\alpha_0(x_0)$ is represented with the following equation (3),

$$\begin{cases} \frac{D\alpha}{Dt} = \frac{\partial \alpha(x,t)}{\partial t} + v(x,t) \cdot \nabla \alpha(x,t) = 0 \\ \alpha(x,0) = \alpha_0(x) \end{cases} \tag{3}$$

Let $\phi_0^T(x_0)$ denote the forward flow map function that calculates final position x_t of a particle, given initial position x_0.

The forward flow map between time $0 \leq t \leq T$ is then defined with the equation (4),

$$\begin{cases} \phi_0^T(x_0) = x \\ \frac{dx}{dt} = v(x(t),t) \\ x(0) = x_0 \end{cases} \tag{4}$$

Similarly, let $\phi_T^0(x_t)$ denote the backward flow map function that calculates initial position x_0

of a particle, given final position x_t.

The backward flow map is the inverse of the forward flow map - in other words, it maps final positions to initial positions, backward through time - and is given by the following equation (5),

$$\begin{cases} \phi_T^0(x) = x_0 \\ \frac{dx}{dt} = v(x(t), t) \\ x(0) = x_0 \end{cases} \tag{5}$$

It can be concluded that the tracer value at x_0 at time 0 is equivalent to the tracer value at position x_t at time t, given x_0 and x_t are related by either equation (4) or equation (5), since the passive tracer travels with fluid trajectories and experiences no change. Hence, in conjunction with equation (5), the following equation (6) is yielded,

$$\alpha(x, t) = \alpha_0(\phi_t^0(x)). \tag{6}$$

Thus, the tracer value at position x at time t is equivalent to the initial tracer value at the position resulting from evaluation of the backward flow map from time t to time 0 at position x.

2.2.3 Flow Map Computation and PDE-based Composition

To compute the flow map, equation (3) was utilized with the following equation as an initial condition, which, in essence, sets the initial tracer field in the domain to be each particle's position (*i.e.* the tracer value at a given spatial location is the location itself),

$$\alpha_0(x) = x. \tag{7}$$

When equation (7) is considered together with equation (6), it is implied that,

$$\alpha(x, t) = \alpha_0(\phi_t^0(x)) = \phi_t^0(x). \tag{8}$$

Thus, by solving equation (3) with the initial condition given by equation (7), the backward flow map ϕ_t^0 can be computed. Similarly, the forward flow map ϕ_0^t can also be derived through the same mathematical sequence simply by flipping the temporal index. This is referred to as "PDE-based flow map computation".

As target time intervals increase, the flow map computation becomes increasingly expensive and susceptible to compounding diffusive and dispersive numerical errors. To address these problems of efficiency, expense, and accuracy, the temporal and spatial domains were both discretized, coupled with an interpolation of smaller, discretized flow map computations, to efficiently compute the total flow map. The total time interval, $[0,\ T]$, on which the flow map was calculated was separated into small intervals of duration Δt of the order of a numerical timestep. Individual flow maps over these timesteps were computed independently of each other and composed to obtain the complete flow map over $[0,\ T]$. Interpolation was required to compose the new flow map, filling in gaps in the flow map where exact calculations were not made due to the smaller, individual time intervals used [5].

2.3 Case Study: Source Conditions

Additional factors, *eg.* tracer source, were incorporated in the passive tracer model detailed above (section 2.2) to create a model of oceanic plastic transport that more accurately simulates plastic pollution in the real world. Through the use of our efficiently computed flow maps, the aim was to compare and analyze plastic particle trajectory patterns created by different source locations, *e.g.* along the coast, point source in the ocean, etc. Seven cases were modeled:

- **Case 1**: Uniform source concentration along coastline, no source in the ocean.
- **Case 2**: Point source in the ocean, set to center of flow map spatial domain.
- **Case 3**: Mouth of Merrimack River only.
  - Location: 42.818897°, -70.810399°
  - Flow Rate: 214 m^3/s
- **Case 4**: Mouth of Charles River only.
  - Location: 42.342862°, -71.008445°

  - Flow Rate: 8.6 m^3/s

- **Case 5**: Two point sources on coastline at the mouths of the Merrimack and Charles Rivers, with weighted concentrations based on river flow output.
- **Case 6**: Combination of case 1 and case 5 - Uniform source along coastline, mouths of Merrimack and Charles weighted.
- **Case 7**: Uniform concentration in all ocean areas.

Initial concentration as a tracer value was incorporated after the computation of flow maps for corresponding time intervals. Following equation (9), tracer values were computed and mapped on trajectories of the flow maps.

$$\alpha(x,t) = \alpha(x_0,0) = \alpha_x(x_0). \tag{9}$$

α denotes tracer value, α_x denotes tracer value as position (as is flow map), x denotes position, and subscript 0 denotes initial condition. Equation (9), in essence, states that the tracer value of a particle at a given position and time is equal to the tracer value of the particle at initial position at time 0, which is also equal to the position value of the particle at initial position.

2.4 Diagram Analysis

In all produced diagrams of plastic movement and distribution, subfigures A through D display plastic distributions based on simulated data from the 20-day period in June 2001: subfigure A shows initial distribution, subfigure B shows distribution at time $t = 1$ day, subfigure C shows distribution at time $t = 7$ days, and subfigure D shows distribution at time $t = 20$ days. Subfigure E displays plastic distribution at time $t = 5$ days based on simulated data from the 5-day period in July 2019. Subfigures A through D are of lower resolution and subfigure E is of higher resolution for contrast in detail and results analysis. In the source concentration cases (figures 4 through 10), colors denote relative tracer concentrations, with red being the highest concentration and blue being the lowest concentration.

In the flow maps (figures 2 and 3) shown below, colors denote initial position, as that is the established tracer value used to develop the flow maps themselves. These flow maps provide a ref-

erence for interpretation of tracer diagrams: the colors indicate initial conditions. For example, in figure 2 and figure 3, the colors denote the final x-positions and y-positions of the fluid, respectively, separated into banded groups. In subfigure D of both figures, the colors thus indicate where each parcel of fluid will end up when corresponded to the bands of subfigure A. This method of interpretation is utilized throughout all diagram analyses in this study.

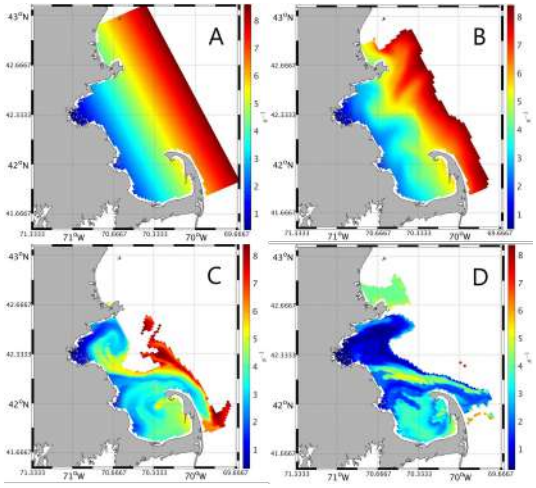

Figure 2: Backward flow map displaying particle movement in the x-direction. Subfigures A, B, C, and D display flow patterns at time $t = 0$, $t = 1$ day, $t = 7$ days, and $t = 20$ days, respectively, with the June 2001 dataset. (Diagrams by competition entrant)

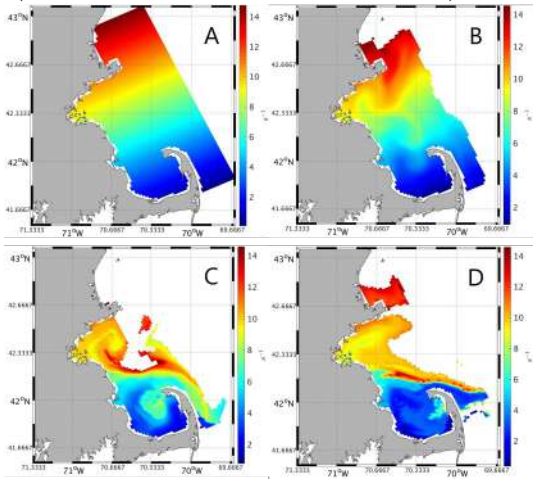

Figure 3: Backward flow map displaying particle movement in the y-direction. Subfigures A, B, C, and D display flow patterns at time $t = 0$, $t = 1$ day, $t = 7$ days, and $t = 20$ days, respectively, with the June 2001 dataset. (Diagrams by competition entrant)

3 Results

3.1 Case 1: Coastal Source

Plastics originating along the coast, as shown in figure 4 below, exhibit a sink region near the Boston Harbor and a void in the center of Cape Cod Bay, shown by the high concentration of red and light blue coloring in the Boston Harbor and a lack thereof in Cape Cod Bay. At 20 days, subfigure D shows the "hook" of Cape Cod Bay surrounded by red coloring, indicating high plastic concentrations; however, the interior of the Bay is relatively empty, showing mostly dark blue coloring with spots of red and light blue. Within short periods of time (a day to a week, shown by subfigures B and C), however, plastics originating near the coast mostly remain near the coast, supported by subfigure E with higher resolution data at 5 days and similar patterns. A sink appears near Boston Harbor while a void appears in Cape Cod Bay, supported by all subfigures, likely due to the movement of fluids as shown in the flow maps developed (figures 2 and 3) and the origin location of plastic particles.

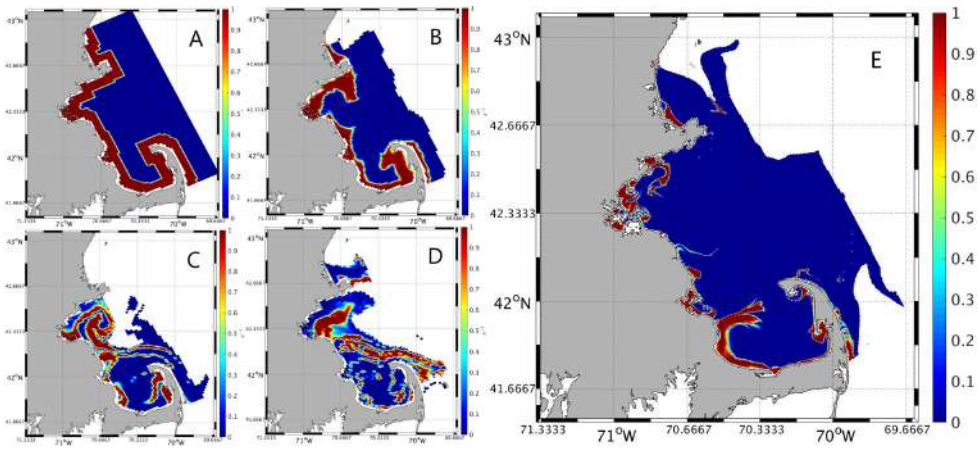

Figure 4: Particles of coastal origin (case 1) display a tendency to cluster in Boston Harbor and disperse outwards from the Bay. Subfigures A, B, C, and D display plastic distribution at time $t = 0$, $t = 1$ day, $t = 7$ days, and $t = 20$ days, respectively, with the June 2001 dataset. Subfigure E displays plastic distribution at time $t = 5$ days with the July 2019 dataset. (Diagrams by competition entrant)

3.2 Case 2: Point Source

A common, though less impactful, source of marine plastic is vessels at sea that discard plastics directly into the water in which they sail. As shown in figure 5 below, point sources tend to remain

mostly together, a beneficial characteristic to be taken advantage of when conducting targeted cleanup efforts. As subfigure E shows, there is slight dispersion at 5 days (that could be assumed to continue after 5 days), a characteristic that subfigures A through D were not able to show due to the lower resolution of the data. The movement of the plastics, however, depends heavily on origin position of the plastics. For this particular case, movement was directed southeast into the Cape Cod Bay, corresponding to patterns displayed in the flow maps (figure 2 and figure 3). This indicates potential of the flow maps to predict non-coastal point source tracer movement, utilizing the cohesive characteristic of concentrated plastic parcels.

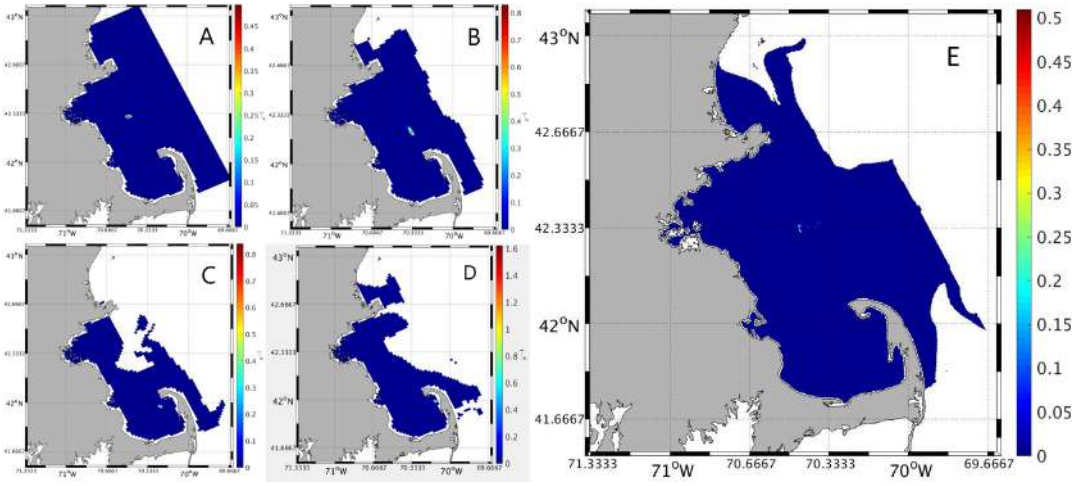

Figure 5: Point sources of plastic (case 2) tend to travel as a mostly-cohesive cluster, simplifying forecast predictions and cleanup efforts. Subfigures A, B, C, and D display plastic distribution at time $t = 0$, $t = 1$ day, $t = 7$ days, and $t = 20$ days, respectively, with the June 2001 dataset. Subfigure E displays plastic distribution at time $t = 5$ days with the July 2019 dataset. (Diagrams by competition entrant)

3.3 Case 3-5: River Discharge

Plastics originating from the Merrimack River, shown in figure 6 below, remained mostly concentrated around the river mouth from days 1 through 20 post-release and dispersed slightly in the longitudinal direction, indicated by the dispersion of colors in that area in subfigure A through D and in subfigure E. Subfigure E, at day 5 (July 2019), displays a clearer dispersion of plastics than subfigure B at day 1 (June 2000), owing to the higher resolution of data. This, however, reveals the relative extent of dispersion, a characteristic useful in directing cleanup efforts.

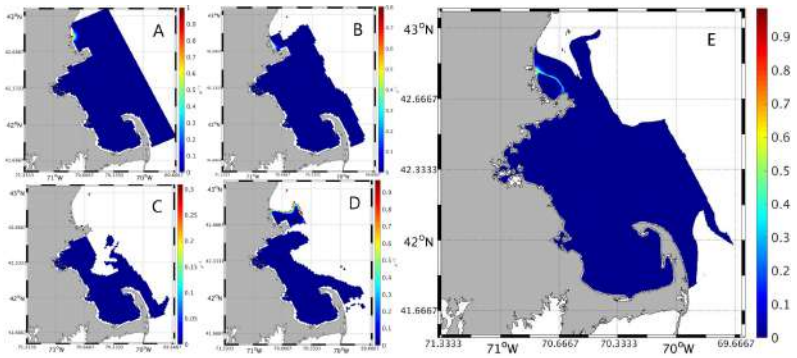

Figure 6: Plastics released from the Merrimack River (case 3) tend to advect outwards slightly. Subfigures A, B, C, and D display plastic distribution at time $t = 0$, $t = 1$ day, $t = 7$ days, and $t = 20$ days, respectively, with the June 2001 dataset. Subfigure E displays plastic distribution at time $t = 5$ days with the July 2019 dataset. (Diagrams by competition entrant)

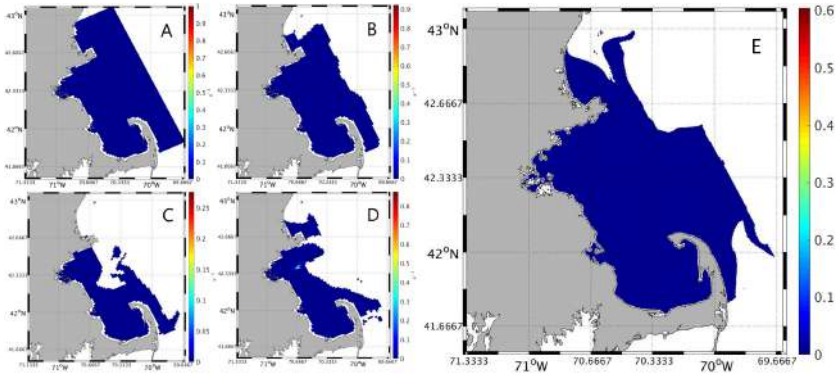

Figure 7: Plastics released from the Charles River (case 4), located in Boston Harbor, tend to remain clustered around the river mouth. Subfigures A, B, C, and D display plastic distribution at time $t = 0$, $t = 1$ day, $t = 7$ days, and $t = 20$ days, respectively, with the June 2001 dataset. Subfigure E displays plastic distribution at time $t = 5$ days with the July 2019 dataset. (Diagrams by competition entrant)

By contrast, plastic released from the Charles River, displayed in figure 7, clustered together and advected outwards as a fairly cohesive individual parcel. The high concentration of plastic eventually ends up at the mouth of the Boston Harbor at twenty days (subfigure D); from a duration of one day through one week, however, the plastic remains very close to the mouth of the Charles River, indicating relatively straightforward direction of possible cleanup efforts. This is supported by the lack of evident coloring in subfigure E: the plastic remains so close to the coast that very little color is visible. The Merrimack River exhibited much wider range in its advection of passive particles

than the Charles River does, particularly at time $t = 20$ days.

Examining the Merrimack River and the Charles River together in the context of plastic pollution (plastic concentrations weighted according to river discharge rates) shows the relative severity of pollution in sink regions identified below (figure 8). The Merrimack River releases a much larger quantity of water — almost 30-fold of the Charles River's output — and most plastic particles originating from that body have high potential to disperse widely outwards after 20 days. As such, cleanup efforts should be conducted as close to major releases as possible. In comparison, the Charles River's output is much smaller and stays near the river mouth; the lack of evident color in subfigure D and the relative size of Boston Harbor's coloring compared to that of the Merrimack region in subfigure E shows how relatively light the pollution is. As the twenty-day diagram (subfigure D) indicates, removal efforts should be targeted to the Merrimack River's plastic release for maximum efficiency. These results mirror the results of figure 6 and figure 7. Thus, the rivers could be modeled separately to yield similar results as if they were modeled together, potentially saving computational power.

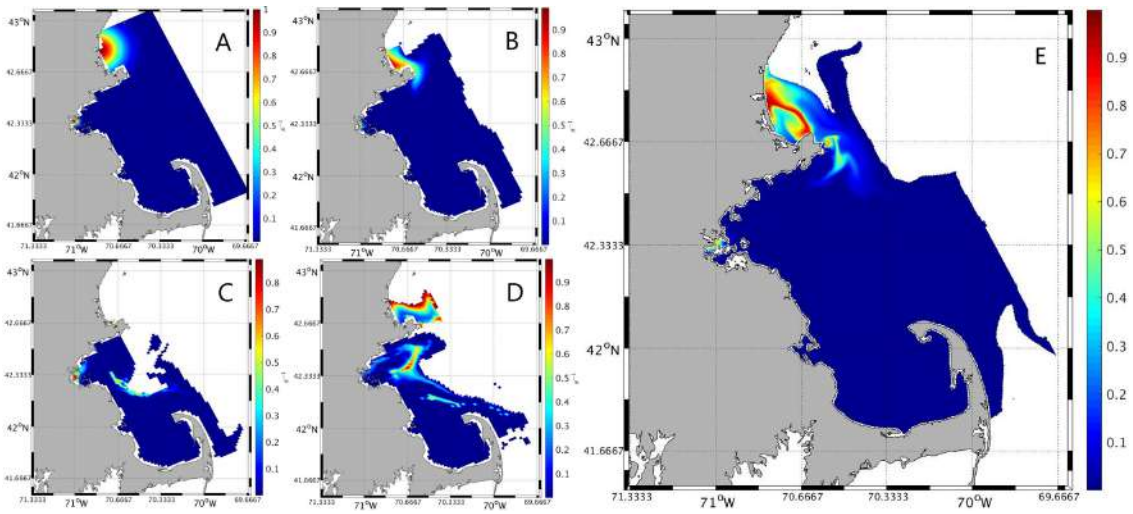

Figure 8: Both the Merrimack River and Charles River modeled together (case 5) shows an dispersion of plastic around the mouth of the Merrimack and an accumulation near the Boston Harbor. Subfigures A, B, C, and D display plastic distribution at time $t = 0$, $t = 1$ day, $t = 7$ days, and $t = 20$ days, respectively, with the June 2001 dataset. Subfigure E displays plastic distribution at time $t = 5$ days with the July 2019 dataset. (Diagrams by competition entrant)

3.4 Case 6: Coastal Sources and River Discharge

Because plastic often originates from many sources simultaneously, a realistic model must include both river and coastal sources for greatest accuracy: in reality, both rivers will be flowing while coastal areas will also be releasing plastic particles due to human population and activity. As shown below in figure 9, the plastics first remain clustered around the coast (subfigure B and subfigure E), but after a week post-release (subfigure C), a sink develops in and around Boston Harbor and a void develops within Cape Cod Bay. This trend continues up to twenty days post-release (subfigure D) with increased dispersion outside of the Bay; however, the greatest cluster of particles remains near Boston Harbor. Individual clusters of plastic decrease in concentration, as shown by the increase in concentration of light blue coloring in subfigure D as compared to subfigure C, where orange coloring indicates higher concentrations than light blue coloring. This suggests that for cleanup efforts to be most efficient, they should be conducted at around a week post-release since the plastic gradually disperses outwards and concentrates less as time continues. In addition, the higher resolution of subfigure E shows detailed distribution much clearer than subfigures A through D, supporting the use of higher resolution and the results obtained by subfigures A through D.

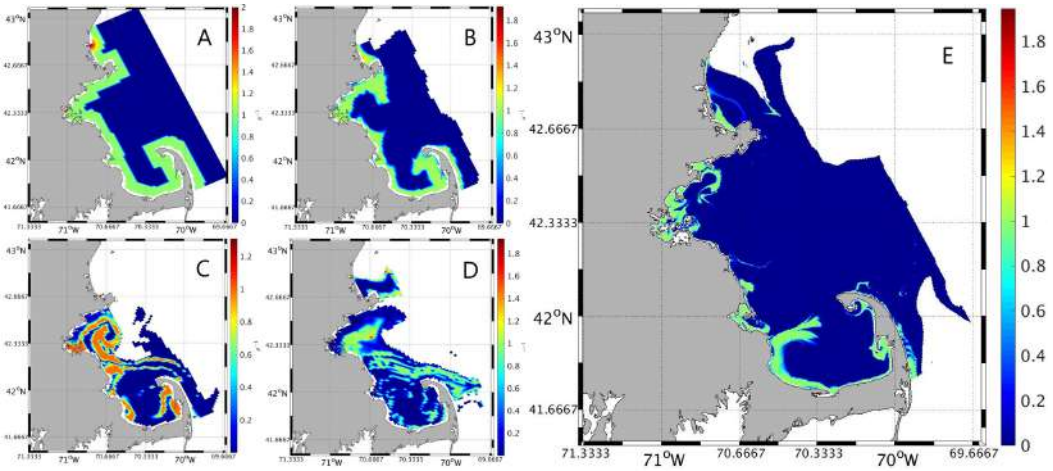

Figure 9: Accounting for release of plastic from both rivers and coastal areas (case 6), the sinks and voids in the above figure present a more comprehensive understanding of real-world plastic pollution. Subfigures A, B, C, and D display plastic distribution at time $t = 0$, $t = 1$ day, $t = 7$ days, and $t = 20$ days, respectively, with the June 2001 dataset. Subfigure E displays plastic distribution at time $t = 5$ days with the July 2019 dataset. (Diagrams by competition entrant)

3.5 Case 7: Uniform Distribution

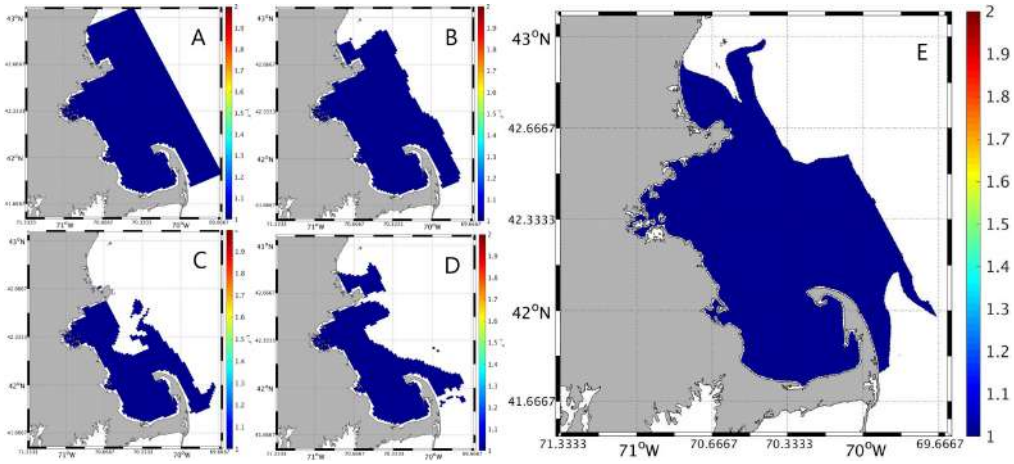

Figure 10: Dark blue indicates the water, which contains equal concentration of plastic in this case, and changes in location of water (case 7). Subfigures A, B, C, and D display plastic distribution at time $t = 0$, $t = 1$ day, $t = 7$ days, and $t = 20$ days, respectively, with the June 2001 dataset. Subfigure E displays plastic distribution at time $t = 5$ days with the July 2019 dataset. (Diagrams by competition entrant)

Assuming uniform initial concentration of particles distributed in all regions of fluid results in a sequence of diagrams that trace fluid movement, a function incredibly helpful in analyzing the containment of particles and thus the true extent of pollution. As evidenced in figure 10 above by the new distribution of dark blue coloring as compared in subfigures B, C, D, and E to subfigure A, fluids tend to remain within Cape Cod Bay, accounting for the retainment of particles within and along the coast of the region. In addition, fluids tend to remain within Boston Harbor, accounting for the trend of the Harbor being a sink for plastic particles. The shrinking size of the target region as time proceeds indicates a loss of fluid, possibly accounting for the dispersion of plastic particles.

4 Discussion

4.1 Massachusetts Bay Flow Patterns

The most striking characteristic of plastic particle trajectories in Massachusetts Bay is the clear accumulation of plastics in and around Boston Harbor, and the consistent lack of particles in the center of Cape Cod Bay. Particles with coastal origins tend generally to cluster around Boston Harbor, leading to a clear sink there and a logical target of plastic particle removal. By contrast,

particles tend to generally scatter closer to the shores of Cape Cod Bay and stay clear of the middle, indicating a general target of Cape Cod shores rather than regions farther into the Bay. Plastics released from rivers tend to first cluster around the mouth of the river within a short period of time and then disperse, hinting at the possible efficacy of a "plastic filter" implemented close to the river mouth or in the general region which could catch and remove macroplastics as they are released. This is particularly true for the Merrimack River, where plastics cluster near the mouth of the river with little movement over 20 days. Finally, point sources tend to stay clustered, allowing for possible tracking and simple collection without concerns about dispersal.

When these general trends, source concentration case results, and flow maps are considered together, it can be seen that the flow maps serve as much of an explanation for trends in plastic trajectories. For example, in the case of plastics of coastal origin, there is a clear void in Cape Cod Bay because no plastic particles are present in the water that flows into the Bay, a conclusion that can be reached by matching the flow map colors to the origins of plastic particles. This is expected, since plastic particles are passive tracers and flow along with fluid without independent influences on their movement. Hence, given just the flow maps, approximations of plastic movement can be generated simply by tracing the movement of water. However, to examine flow patterns while taking into account relative initial concentrations of sources, specific source case trajectory maps must be developed and analyzed (such as those of figures 4 through 10).

Though the two datasets used varied widely in year (2001 and 2019) and in duration (20 days and 5 days), general flow patterns were similar, most likely due to the prevailing wind patterns and ocean currents affecting the studied region (figure 11). The dominant ocean currents within the Massachusetts and North Atlantic region are the North Atlantic Current and Gulf Stream, which carry water towards the northeast (figure 11). This likely accounts for the exiting of plastic particles from the domain near the Merrimack River and the lack of particles entering the Cape Cod Bay (since there is no major current influence there); however, this does not account for the accumulation of plastics around the Boston Harbor or the initial dispersal of plastics from coastal and river origins. These patterns could be accounted for by wind patterns in the region, as stated in a similar study by Lermusiaux et al. [10] which also examined plastic flow in Massachusetts Bay

using a dataset from August 2019. Lermusiaux et al. [10] concluded that winds drive both the initial advection of the plastics as well as the movement of the plastics within the domain and out of the domain. In particular, these winds are dominant during the first three days, which could account for the initial dispersion of plastics.

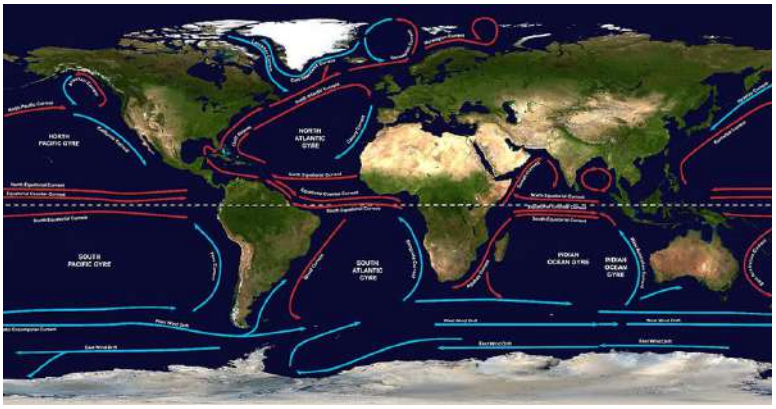

Figure 11: Prevailing ocean currents around the globe. Massachusetts is primarily affected by the North Atlantic Current and Gulf Stream, which direct water northeastward. [11]

The comparison of higher resolution and lower resolution data, through use of two separate datasets, illustrates both the key flow patterns of plastic and the importance of high resolutions in acquiring detailed results. As figures 4 through 10 showed, higher resolution data yieled results that more clearly displayed erratic but small changes in plastic flow. In order to properly address these small fluctuations in plastic flow, higher resolution data must be used.

4.2 Method Analysis

The novel computational model utilized - a Lagrangian model imposed on an Eulerian grid - takes advantage of the benefits of both modeling approaches to create a computationally efficient and numerically accurate model [5].

First, the plotting of flow maps as the basis on which particle advection lay was beneficial. The computation of flow maps allowed for infinite particle trajectories to be determined at the same computational cost of directly computing tracer advection for one spatio-temporal condition. As such, the scope of flow map computation is clearly much broader — in that it allows for many more trajectories to be computed than conventional computational methods do — and has more

implications. For instance, the relatively fast speed of computation allows the model to be changed and applied to different regions rapidly, extending its applications.

Second, the concept of utilizing an Eulerian grid take advantage of the fixed reference perspective, creating an easier grid on which to plot particle trajectories. However, Eulerian computations are highly inefficient; hence, use of Lagrangian methods (which compute LCSs) is much more efficient. This method captures both benefits [5].

Third, the discretization of the temporal domain further increases the computational efficiency of the model, beyond the basic Lagrangian PDE method. This allows for faster computational speed, albeit at the expense of accuracy when time steps are made too large [5]. Larger time steps lead to missed details in trajectory changes, which could lead clean up efforts in the wrong direction. However, this allows for greater user control over the model's processing based on their needs, another benefit of the model.

Most importantly, the main advantage of this novel method is that it is very resistant to numerical diffusion, or the phenomenon of inserting errors in calculations that compromise the accuracy of the computational solution. Hence, by decreasing numerical diffusion, the model is able to achieve better accuracy than conventional methods [5].

4.3 Model Application

Because the current model was developed from a passive tracer model, its implications are much wider than simply plastic. Thus far, no plastic-specific factor has been included in the model's computations; hence, the model could represent any passive particle (*e.g.* oil, larvae, dye, etc.) and is widely applicable in many areas of pollution control, forecasting, and prevention. In addition, because the velocity field is an external matrix on which the model is run, the model can easily be applied to other regions with pollution problems, simply by changing the velocity field matrix on which the model is implemented. This widens the application of the model.

The development of forward and backward flow maps, on which tracer advection is mapped, allows for dual function of the model for both forecasting and backcasting. In essence, the model could both predict where particles will be at time t given their initial position at time $t = 0$ and determine where particles originated from given their final position at time t. In the context of

pollution control, this duality is extremely useful. Known sources of pollution could be tracked and particles could be removed with the forecasting function, while particles with unknown sources could be backtracked to target pollution at its source.

5 Conclusion and Future Work

A numerical model of plastic particle transport in Massachusetts Bay was successfully developed to better understand plastic pollution during specific time periods (June 2001 and July 2019) through the mapping of particle trajectories. A novel modeling methodology was utilized, combining Lagrangian flow characteristics (LCS mapping) and Eulerian fixed reference grids. With this combination, computational time and expense was decreased, increased computational efficiency, and created a more accurate model with the ability to both forecast and backcast, functions which are useful for predicting and preventing plastic pollution. Realistic initial source conditions were incorporated to specialize the model for plastic pollution.

The model could be improved in several ways. Firstly, there is currently no method of validating the true accuracy of the model due to a lack of real-world data taken during the corresponding time periods. Thus, it would be useful to collect field data using buoys and collection systems in addition to forecasting using the developed model, which would allow for the calibration of the model and validation of its accuracy. Secondly, marine plastic particles have many characteristics that affect their transport through the ocean, such as density (settling and sinking), size (macroplastics, microplastics, mesoplastics), tendency to fragment into smaller pieces, and biological and chemical interactions with marine organisms and ocean water. Incorporation of these factors into the model for more accurate results could be achieved utilizing more comprehensive transport PDEs, hence increasing the model's accuracy and specificity for plastics. Lastly, this model could be applied to other regions of the world for better understanding of plastic pollution and for a broader application.

References

[1] L. C.-M. Lebreton, S. D. Greer, and J. C. Borrero. Numerical modelling of floating debris in the world's oceans. *Marine Pollution Bulletin*, 64(3):653–661, Mar 2012.

[2] K. L. Law. Plastics in the marine environment. *Annual Review of Marine Science*, 9:205–229, Jan 2017.

[3] L. Lebreton, B. Slat, F. Ferrari, B. Sainte-Rose, J. Aitken, R. Marthouse, S. Hajbane, S. Cunsolo, A. Schwarz, A. Levivier, and et al. Evidence that the great pacific garbage patch is rapidly accumulating plastic. *Scientific Reports*, 8(1), 2018.

[4] A. Cozar, F. Echevarria, J. I. Gonzalez-Gordillo, X. Irigoien, B. Ubeda, S. Hernandez-Leon, A. T. Palma, S. Navarro, J. Garcia-de Lomas, A. Ruiz, and et al. Plastic debris in the open ocean. *Proceedings of the National Academy of Sciences of the United States of America*, 111(28):10239–10244, Jul 2014.

[5] C. S. Kulkarni and P. F. Lermusiaux. Advection without compounding errors through flow map composition. *Journal of Computational Physics*, Jun 2019.

[6] X. Zhang, Z. Chen, and Y. Liu. *The material point method: a continuum-based particle method for extreme loading cases*. Elsevier, 2017.

[7] R. K. Jain, Z. C. Cui, and J. K. Domen. Environmental impacts of mining. *Environmental Impact of Mining and Mineral Processing*, page 53–157, 2016.

[8] S. Prants, M. Budyansky, V. Ponomarev, and M. Uleysky. Lagrangian study of transport and mixing in a mesoscale eddy street. *Ocean Modelling*, 38(1-2):114–125, Feb 2011.

[9] S. Liubartseva, G. Coppini, R. Lecci, and E. Clementi. Tracking plastics in the mediterranean: 2d lagrangian model. *Marine Pollution Bulletin*, 129(1):151–162, Feb 2018.

[10] P. Lermusiauxa, A. Guptaa, C. Kulkarnia, G. Flierla, J. Marshalla, and T. Peacocka. Plastic pollution in the coastal oceans: Characterization and modeling.

[11] NOAA. What is a gyre?, 2018. Accessed: 2019-11-8.